



# UV and bacteriophages as a chemical-free approach for cleaning membranes from anaerobic bioreactors

Giantommaso Scarascia<sup>a</sup> , Luca Fortunato<sup>a</sup> , Yevhen Myshkevych<sup>a</sup> , Hong Cheng<sup>a</sup>, TorOve Leiknes<sup>a</sup>, and Pei-Ying Hong<sup>a,1</sup>

<sup>a</sup>Water Desalination and Reuse Center, Biological and Environmental Science & Engineering Division, King Abdullah University of Science and Technology, Thuwal 23955-6900, Saudi Arabia

Edited by Manish Kumar, The University of Texas at Austin, Austin, TX, and accepted by Editorial Board Member Pablo G. Debenedetti January 16, 2021 (received for review August 5, 2020)

**Anaerobic membrane bioreactor (AnMBR) for wastewater treatment has attracted much interest due to its efficacy in providing high-quality effluent with minimal energy costs. However, membrane biofouling represents the main bottleneck for AnMBR because it diminishes flux and necessitates frequent replacement of membranes. In this study, we assessed the feasibility of combining bacteriophages and UV-C irradiation to provide a chemical-free approach to remove biofoulants on the membrane. The combination of bacteriophage and UV-C resulted in better log cells removal and ca. 2× higher extracellular polymeric substance (EPS) concentration reduction in mature biofoulants compared to either UV-C or bacteriophage alone. The cleaning mechanism behind this combined approach is by 1) reducing the relative abundance of *Acinetobacter* spp. and selected bacteria (e.g., *Paludibacter*, *Pseudomonas*, *Cloacibacterium*, and gram-positive Firmicutes) associated with the membrane biofilm and 2) forming cavities in the biofilm to maintain water flux through the membrane. When the combined treatment was further compared with the common chemical cleaning procedure, a similar reduction on the cell numbers was observed (1.4 log). However, the combined treatment was less effective in removing EPS compared with chemical cleaning. These results suggest that the combination of UV-C and bacteriophage have an additive effect in biofouling reduction, representing a potential chemical-free method to remove reversible biofoulants on membrane fitted to an AnMBR.**

biofouling | bacteriophage | UV | anaerobic processes | wastewater

Anaerobic membrane bioreactor (AnMBR) has emerged as an energy-efficient biotechnology for municipal wastewater treatment (1). AnMBR can be used to clean wastewater of various organic concentrations, which is represented by chemical oxygen demand (COD) per volume of wastewater per day, and result in energy recovery from the wastewater. To exemplify, a laboratory-scale AnMBR was able to remove up to 98% of a wide range of 0.8 to 10 g COD per L wastewater (2). The organic carbon in wastewater is fermented to produce methane, which can be combusted and converted to electrical energy. Anaerobic mode of wastewater treatment further eliminates the need for aeration, hence saving up to 75% of the energy costs associated with conventional wastewater treatment (3). Besides low energy costs, the post-AnMBR effluent has low turbidity, retains the ammonium and phosphate, and can potentially be reused as liquid fertilizers for agricultural crops (4). Furthermore, anaerobic process results in lower sludge production than aerobic treatment, therefore minimizing solid waste disposal costs (1, 5). Finally, the coupling of membrane to anaerobic fermentation tanks reduces the required footprint for wastewater treatment process by eliminating the need for clarifiers (6, 7).

Despite these advantages, similar to other types of MBR technologies, AnMBR is prone to membrane biofouling due to the unwanted deposition of microorganisms and their extracellular polymeric substances (EPS) on the membrane surface (8). This deposition of biofoulants decreases the operational flux and rapidly increases the transmembrane pressure (TMP) and energy

required to maintain a constant flux (9). Membranes typically account for 10 to 30% of the total operational costs of MBRs (10). Therefore, frequent replacement of fouled membranes can significantly add on to the overall costs associated with using such biotechnology to clean wastewater.

Current strategies to reduce membrane biofouling include the use of physical means (e.g., gas scouring, backwashing, and sonication) and chemical cleaning [e.g., citric acid and chlorine (6)]. Physical cleaning is generally more effective to remove the reversible foulant layer (11), but the use of hydraulic or mechanical forces to clean the membrane can increase energy costs depending on the cleaning frequencies and regimes (12). Current physical cleaning approaches are also used to complement chemical cleaning which is effective against irreversible foulant layers (13). However, the use of chemicals should be limited to a minimum frequency since repeated chemical cleaning may detrimentally impact the membrane integrity, and disposal of the spent chemicals can pose health, safety, and environmental concerns (14). In addition, it was shown that certain bacteria such as *Acinetobacter* spp. are strongly resistant to chemical disinfectants (15).

Biological-based approaches have emerged as interesting options to alleviate membrane biofouling (16, 17). In particular, bacteriophages are viruses that infect viable bacteria and have been used against biofilm-associated bacteria for clinical therapeutic treatments (18–20). Besides infecting their intended

## Significance

**Anaerobic membrane bioreactors (AnMBR) can clean wastewater at lower energy costs and produce high-quality effluent for nonpotable reuse. However, biofouling represents the main bottleneck for membrane filtration efficiency. Biofouling is commonly reduced through chemical treatment. These agents are often detrimental for the environment and health safety due to the formation of toxic byproducts. Therefore, we present a new approach, based on the additive antifouling action of bacteriophages infection and UV-C irradiation, to reduce anaerobic membrane biofouling. This new strategy could potentially delay the occurrence of membrane fouling by removing the reversible fouling layers on membranes, in turn reducing the frequencies and amount of chemicals needed throughout the course of wastewater treatment.**

Author contributions: G.S. and P.-Y.H. designed research; G.S., L.F., Y.M., and H.C. performed research; T.L. and P.-Y.H. contributed new reagents/analytic tools; G.S., L.F., Y.M., and P.-Y.H. analyzed data; and G.S. and P.-Y.H. wrote the paper.

The authors declare no competing interest.

This article is a PNAS Direct Submission. M.K. is a guest editor invited by the Editorial Board.

Published under the PNAS license.

<sup>1</sup>To whom correspondence may be addressed. Email: peiyong.hong@kaust.edu.sa.

This article contains supporting information online at <https://www.pnas.org/lookup/suppl/doi:10.1073/pnas.2016529118/-DCSupplemental>.

Published September 7, 2021.

bacterial host, bacteriophages can also induce the release of enzymes that degrade the EPS biofilm matrix, in turn, increasing biofilm susceptibility to biocides (21). Moreover, bacteriophages are able to infect bacteria over a broad range of pH, salinity, and temperature (22). For these reasons, bacteriophages were also applied as a biological-based approach to reduce membrane biofouling (23–25). However, most of the early studies utilized only single-species (e.g., *Pseudomonas aeruginosa* or *Delftia tsuruhatensis*) or simple multispecies biofilm (e.g., *P. aeruginosa* in combination with *Acinetobacter johnsonii* and *Bacillus subtilis*) and demonstrated ca. <1-log improvement in cell number reduction or flux recovery (22, 25). Despite these promising demonstrations of using bacteriophages against membrane fouling, the effectiveness of bacteriophages against a complex biofilm has not been demonstrated and is anticipated to be rather challenging. This is because the variety of microorganisms in a complex biofilm goes against the high specificity of phage infection. In addition, bacteriophages may face limited diffusion or penetration through the complex biofilm before encountering and infecting their host.

To improve the efficacy of bacteriophages against membrane biofilm, we demonstrated here the use of bacteriophages in combination with UV (UV-C) irradiation. UV-C (254 nm) imposes germicidal effect by causing DNA damage, and it has been widely used for effluent disinfection (26) and for wastewater pretreatment (27). Although UV effect on biofilm was investigated earlier, these studies were dedicated to determine its antibiofilm action within the water distribution system (28, 29) and not for the purpose of mitigating membrane biofouling. By applying bacteriophages together with UV-C irradiation to tackle membrane biofouling, we hypothesize that these two agents can have an additive action against the biofilm matrix. This is because UV-C irradiation was determined previously to trigger bacteriophages to enter into lytic mode and lyse planktonic bacterial cells (30), but such demonstrations on the use of UV-C to enhance the efficiency of bacteriophage against the biofilm matrix have not been conducted.

In this study, we aim to demonstrate the use of bacteriophages in combination with UV-C to reduce membrane biofouling in AnMBR. *Acinetobacter* was previously determined to be a core membrane-associated bacterial genus in AnMBR and was present at a high relative abundance ranging from 3 to 4% of total microbial community (31). In the case of AnMBR, the biofilm microbial community was revealed to assemble based on random stochastic events. However, a few core genera including *Acinetobacter* occurred in relative abundance that deviated from the neutral assembly model (31). This suggests that *Acinetobacter* may be playing a potential keystone role in the formation of biofouling layers on the membrane of AnMBR and can be potential target to eliminate in a bid to alleviate membrane biofouling. Hence, a mixture of three isolated *Acinetobacter* spp. bacteriophages was applied in combination with UV-C exposure, and its effect on the membrane biofouling layer was analyzed and compared against individual treatment with bacteriophages or UV-C alone. The cleaning mechanisms are further elucidated by means of 16S rRNA amplicon sequencing of active microbial community and optical coherence tomography (OCT). The treatment combining bacteriophages and UV-C was also compared against the chemical cleaning method to examine its feasibility as an alternative biological-based approach to reduce AnMBR biofouling.

## Results

### Isolated Bacteriophages and Their Ability to Infect Membrane Biofilm.

*Acinetobacter junii*, *Acinetobacter modestus*, and *Acinetobacter seohaensis* were isolated from wastewater during our routine wastewater monitoring surveillance. Considering the presence of these three species representing *Acinetobacter* genus in wastewater,

bacteriophages targeting them were subsequently isolated from the influent of the King Abdullah University of Science and Technology (KAUST) wastewater treatment plant and then characterized based on their morphology. All three bacteriophages showed regular icosahedral head with no visible tail. The size of the head was ~86 nm for *A. junii* phage (SI Appendix, Fig. S1A), ~75 nm for *A. modestus* phage (SI Appendix, Fig. S1B), and ~68 nm for *A. seohaensis* phage (SI Appendix, Fig. S1C). Based on the Ackermann classification (32), the three bacteriophages isolated in this study could tentatively be placed in the order *Caudovirales*, under the *Podoviridae* family, constituted by an icosahedral head and short or absent tail. Each isolated phage showed high specificity to infect only its direct host (SI Appendix, Figs. S2–S4).

An AnMBR was set up and fed with synthetic wastewater. Three membranes were connected to the bioreactor in parallel and were operated in crossflow mode (SI Appendix, Fig. S5). The three membranes were harvested at TMPs of 20, 40, and 60 kPa (with  $\pm 2$  kPa SD in measurements for each TMP). Membranes were then harvested, divided in pieces, and treated ex situ with our test conditions.

The mixture of *A. modestus*, *A. junii*, and *A. seohaensis* bacteriophages were introduced either alone or in combination with UV-C to the fouled membranes harvested at the three different TMPs. One piece of each membrane was not treated and used as a control. The entire experiment involving the different cleaning strategies at each TMP was repeated in biological triplicates (i.e.,  $n = 3$  for control;  $n = 3$  for each type of cleaning strategy). All experiments were conducted at a multiplicity of infection (MOI) of 1. MOI of 1 was chosen as there was no significant difference in how the hosts' specific growth rates were affected by MOI of 0.01, 0.1, and 1 compared to control (one-way ANOVA,  $P > 0.05$ ; SI Appendix, Fig. S6). MOI of 5 was able to affect *A. seohaensis* better than at the other MOIs but did not outperform when used to infect the other two *Acinetobacter* hosts (SI Appendix, Fig. S6).

Plaque forming unit (PFU) count was performed in triplicate after each treatment. All three bacteriophages, in the absence of UV-C, increased in their PFUs compared to the initial spiked amount when introduced to membranes harvested at ca. 40 and 60 kPa (SI Appendix, Fig. S7;  $P < 0.04$ ). However, only *A. modestus* bacteriophage was able to actively propagate when introduced to membranes harvested at  $20 \pm 2$  kPa (SI Appendix, Fig. S7B;  $P = 0.03$ ), while the rest of the phages did not have PFUs that were statistically different from the initial spiked value (SI Appendix, Fig. S7A and C). In contrast, UV-C + bacteriophages treatment did not result in any increase in PFU numbers of both *A. junii* and *A. seohaensis* bacteriophages for all membranes harvested at ca. 20, 40, and 60 kPa (SI Appendix, Fig. S6A and C). Only *A. modestus* phage increased in its PFU despite the presence of UV-C, and the final PFU numbers were significantly higher compared with the initial value spiked to the membranes harvested at ca. 40 and 60 kPa (SI Appendix, Fig. S7B;  $P < 0.001$ ).

**Biofilm Analysis: Bacterial Cells.** Bacterial cell enumeration at different sections of a membrane harvested at  $40 \pm 2$  kPa was first performed to assess biofilm homogeneity. The results in SI Appendix, Table S1, indicate the number of cells was always in a similar order of magnitude, ranging ca.  $10^9$  cells per  $\text{cm}^2$  throughout the membrane surface. This allowed us to divide the same membrane into equal portions for comparison of treatment efficacy.

To assess the effect of the different treatments on membrane biofilm, the number of cells was counted in three biological replicates at each treatment condition and TMP. Compared with the control, the bacteriophage mixture alone significantly reduced the number of cells associated with the biofilm from  $40 \pm 2$  kPa membrane (Fig. 1A;  $P = 0.02$ ). The same reduction did not occur for membranes harvested at ca. 20 and 60 kPa ( $P > 0.15$ ). Both UV-C and UV-C + bacteriophages treatment significantly

reduced the number of cells compared to the control for membranes harvested at all biofouling rates analyzed in this study (Fig. 1A;  $P < 0.0001$ ). In particular, UV-C + bacteriophage treatment was able to outcompete the UV-C-only treatment for membranes harvested at ca. 40 and 60 kPa (Fig. 1A;  $P < 0.0001$ ), with the UV-C + bacteriophage treatment reporting up to  $1.36 \log \pm 0.05 \log$  (calculated on three replicates) reduction of cells compared with the control. However, there was no statistical difference between the UV-C + bacteriophage treatment and the UV-C only treatment for membranes harvested at  $20 \pm 2$  kPa (Fig. 1A;  $P = 0.99$ ).

Dead and alive biofilm cell ratio was calculated after the application of the treatments on the harvested membranes. Similar trends were observed for the ratio between alive and dead cells in the biofilm. For membranes harvested at ca. 40 and 60 kPa, bacteriophage mixture ( $P < 0.01$ ), UV-C only ( $P < 0.0001$ ), and UV-C + bacteriophage ( $P < 0.0001$ ) were able to reduce the alive to dead cell ratio compared to the control (Table 1). UV-C + bacteriophage had a significantly lower ratio compared to UV-C only for membranes harvested at ca. 40 and 60 kPa ( $P < 0.0001$ ), while there was no difference between these two treatments for membranes harvested at  $20 \pm 2$  kPa (Table 1;  $P = 0.66$ ). Moreover, there was no difference between control and bacteriophages treatment ( $P = 0.47$ ) for membrane harvested at  $20 \pm 2$  kPa while the UV-C + bacteriophage and UV-C-only treatments had the same significant effect on the alive to dead cells ratio compared to the control (Table 1;  $P < 0.0001$ ).

**Biofilm Analysis: ATP.** ATP concentration at different conditions within the biofilm matrix was used as an indicator of cell activity. The maximum cell activity for the control was observed for membranes harvested at  $40 \pm 2$  kPa (Fig. 1B). For membranes harvested at ca. 40 and 60 kPa ( $n = 3$  at each TMP), ATP concentration was significantly reduced by  $14 \pm 3.2$  and  $9 \pm 1.8 \mu\text{M}/\text{cm}^2$ , respectively, due to bacteriophage application compared to the control (Fig. 1B;  $P < 0.0009$ ). This difference was, however, not observed for membranes harvested at  $20 \pm 2$  kPa ( $n = 3$ ;  $P = 0.74$ ). UV-C and UV-C + bacteriophages reduced

**Table 1. Ratio between alive and dead cells in membrane biofilm after different treatments and at different biofouling rates**

Condition	20 kPa	40 kPa	60 kPa
Control	$1.22 \pm 0.11$	$1.05 \pm 0.02$	$1.15 \pm 0.10$
Bacteriophage	$1.17 \pm 0.13$	$0.84 \pm 0.05$	$1.01 \pm 0.10$
UV-C	$0.5 \pm 0.09$	$0.48 \pm 0.08$	$0.56 \pm 0.08$
UV-C + bacteriophage	$0.53 \pm 0.14$	$0.24 \pm 0.05$	$0.25 \pm 0.09$

The data are presented as average ( $n = 3$ )  $\pm$  SD.

ATP concentration for all membranes compared with the control (Fig. 1B;  $P < 0.0001$ ). Specifically, UV-C + bacteriophages outcompeted UV-C treatment alone when the membrane was harvested at ca. 40 and 60 kPa (Fig. 1B;  $P < 0.003$ ), achieving a total reduction of at least  $40 \pm 3.0 \mu\text{M}/\text{cm}^2$  compared with the control.

#### Biofilm Analysis: Proteins and Polysaccharides in Biofilm Matrix.

Proteins and polysaccharides in the EPS fraction of the biofilm were quantified at different conditions for membrane harvested at ca. 20, 40, and 60 kPa ( $n = 3$  for each TMP). All treatments (i.e., bacteriophages, UV-C, and UV-C + bacteriophage) caused a reduction in both biofilm-associated proteins and polysaccharides concentration on membranes harvested at ca. 40 and 60 kPa compared to control ( $n = 3$ ; Fig. 2;  $P < 0.0002$ ). The bacteriophage treatment did not result in any significant reduction in both proteins and polysaccharides concentration on membranes harvested at  $20 \pm 2$  kPa ( $n = 3$ ;  $P = 0.37$ ). In contrast, UV-C and UV-C + bacteriophages treatments reduced at least 50% of proteins and 35% of polysaccharides concentrations compared with the control across all tested membranes (Fig. 2). In particular, for membranes harvested at ca. 40 and 60 kPa ( $n = 3$  each), UV-C + bacteriophages treatment achieved a statistically higher proteins and polysaccharides reduction compared with UV-C-only treatment (Fig. 2;  $P < 0.004$ ), while the

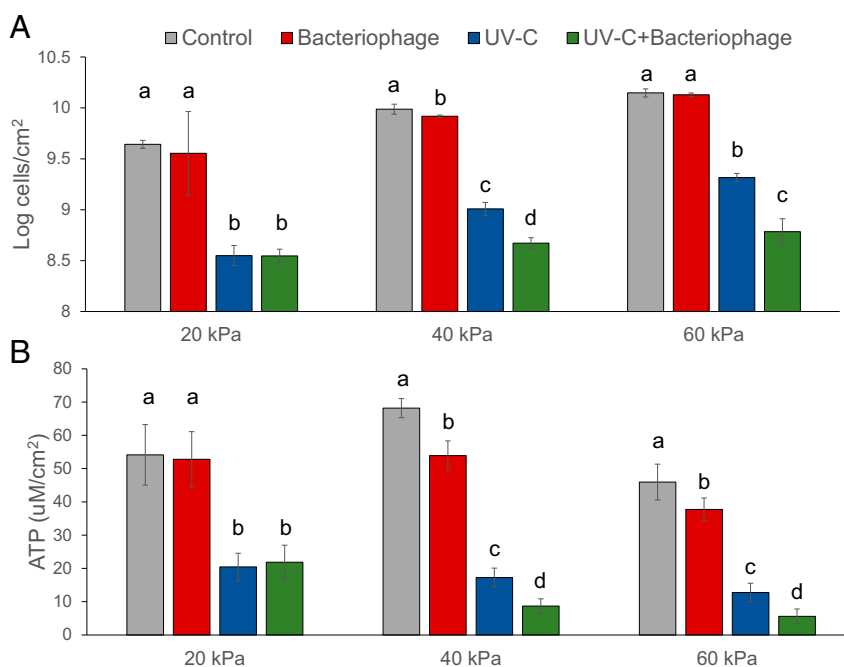


**Fig. 1. (A)** Log number of cells and **(B)** ATP concentration in the membrane biofilm after each treatment at each biofouling rate. Error bars indicate SD among the three replicates. Within the same biofouling rate, bars indicated with different letters are statistically different from each other.



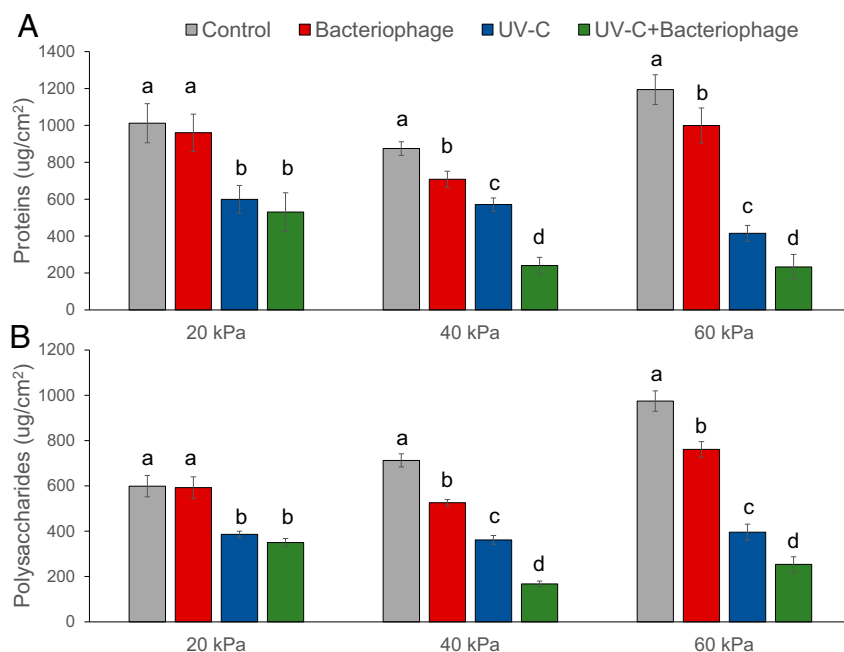


**Fig. 2.** (A) Protein and (B) polysaccharide concentrations in the membrane biofilm after each treatment at each biofouling rate. Error bars indicate SD among the three replicates. Within the same biofouling rate, bars indicated with different letters are statistically different from each other.

difference was not significant for the membranes harvested at  $20 \pm 2$  kPa ( $P > 0.24$ ).

**Active Bacterial Community Characterization.** Considering that there was a difference in cell numbers, ATP, protein, and polysaccharide concentrations due to treatment, the cleaning mechanism was further elucidated by first understanding what bacterial populations were removed by the respective treatment conditions. To achieve this, RNA was extracted from the biofilm harvested at ca. 20, 40, and 60 kPa and exposed to each treatment ( $n = 3$  for each TMP and for each treatment). RNA was then reverse-transcribed into cDNA, amplified for the 16S rRNA gene and sequenced by Illumina MiSeq. The data were used to calculate the relative abundance of the active bacterial community at genus level. Genus *Acinetobacter* was the intended target of the isolated bacteriophages, and its relative abundance was reduced significantly across all tested membranes compared with the control when bacteriophages were applied alone or in combination with UV-C (Table 2). Although not the intended target of the isolated bacteriophages, other genera were also affected in their relative abundance. For example, the relative abundance of genus *Pseudomonas* was significantly lower upon bacteriophages and UV-C + bacteriophages treatments but increased in its relative abundance upon UV-C-only treatment (Table 2). Moreover, two anaerobic gram-negative genera *Paludibacter* and *Cloacibacterium* also reduced in their relative abundance upon bacteriophages and UV-C + bacteriophage treatment. A similar observation was made for gram-positive bacteria which had a lower relative abundance compared to control upon exposure to bacteriophage and UV-C + bacteriophage (Table 2). UV-C treatment, however, resulted in an increase in the relative abundance for most gram-positive bacteria compared to the control, particularly for membranes harvested at  $40 \pm 2$  kPa.

**OCT Analysis.** To further elucidate the cleaning mechanism, we used OCT (33) to perform in situ noninvasive biomass analysis. Results from OCT would allow assessment on how different treatments affect the membrane biofilm structure. For this

analysis, AnMBR membrane was harvested at  $40 \pm 2$  kPa, which is a TMP representative of medium fouling extent. The membrane portions were exposed to three different treatments and in the control condition prior to observations under OCT. Fig. 3 shows an upper view of the three-dimensional (3D) cross-sections of the different treatments employed in this study. There was an observed change in the biofilm coverage across the membrane. For example, control sample presented a flat and compact biomass structure that was homogeneously distributed on the membrane surface (Fig. 3A). At the end of the exposure, all the treatments led to a partial reduction of the biofilm coverage on the membrane and a more irregular morphology in terms of thickness and roughness (Fig. 3 and *SI Appendix, Table S2*). There was at least 11.5% reduction in biofilm coverage compared to the control as a result of the treatments. In addition, a decrease of 20% of biovolume was observed after 6 h exposure to all the treatments compared with the control (*SI Appendix, Table S2*;  $P < 0.0001$ ).

Bacteriophage infection alone was further monitored over time in terms of biofilm removal. It was observed that a substantial decrease in biovolume and increase in roughness was observed already after 1 h from the beginning of the bacteriophage treatment (*SI Appendix, Table S3*). A further decrease in biovolume and increase in roughness was observed after 3 h, albeit at a lower extent than that observed in the first hour (*SI Appendix, Table S3*).

**Effect of the Order of Application of UV-C and Bacteriophages.** UV-C was applied independently before bacteriophages addition to assess if this order of application will be equally effective in biofilm removal. This order of applying UV-C and bacteriophage is subsequently referred to as “independent UV-C + bacteriophages” treatment. It was observed that UV-C + bacteriophages treatment resulted in statistically higher cells removal (*SI Appendix, Fig. S8A*;  $P = 0.01$ ) and polysaccharides concentration reduction (*SI Appendix, Fig. S8B*;  $P = 0.02$ ) compared to the independent UV-C + bacteriophage treatment. However, there was no statistical difference in the reduction of protein concentration ( $P = 0.72$ ) achieved by either treatment.

**Table 2. Percentage relative abundance for different genera in control and upon exposure to treatment**

Genus	Control	Bacteriophages	UV-C	UV-C + bacteriophages
<b>20 kPa</b>				
<i>Micrococcus</i> <sup>†</sup>	0.03 ± 0.02	0.00 ± 0.00*	0.04 ± 0.04	0.00 ± 0.00*
<i>Cloacibacterium</i>	0.09 ± 0.02	0.01 ± 0.00*	0.10 ± 0.02	0.01 ± 0.00*
<i>Paludibacter</i>	0.40 ± 0.08	0.22 ± 0.14	0.54 ± 0.11	0.40 ± 0.22
<b><i>Acinetobacter</i></b>	6.04 ± 0.94	0.01 ± 0.01*	7.58 ± 0.31**	0.02 ± 0.01*
<i>Pseudomonas</i>	4.67 ± 1.32	0.44 ± 0.17*	5.27 ± 1.42	0.50 ± 0.21*
<i>Unclassified_Firmicutes</i> <sup>†</sup>	1.56 ± 0.71	0.41 ± 0.50*	1.49 ± 0.92	0.57 ± 0.45*
<i>Unclassified_Clostridiales</i> <sup>†</sup>	0.12 ± 0.02	0.07 ± 0.01*	0.13 ± 0.04	0.08 ± 0.03
<i>Unclassified_Clostridiaceae</i> <sup>†</sup>	0.03 ± 0.01	0.02 ± 0.01	0.04 ± 0.02	0.02 ± 0.01
<i>Clostridium sensu stricto</i> <sup>†</sup>	0.05 ± 0.03	0.02 ± 0.01	0.09 ± 0.03**	0.02 ± 0.01
<b>40 kPa</b>				
<i>Micrococcus</i> <sup>†</sup>	0.04 ± 0.00	0.00 ± 0.00*	0.08 ± 0.02**	0.00 ± 0.00*
<i>Cloacibacterium</i>	0.10 ± 0.01	0.01 ± 0.00*	0.11 ± 0.03	0.01 ± 0.01*
<i>Paludibacter</i>	0.42 ± 0.02	0.22 ± 0.14*	0.51 ± 0.11	0.13 ± 0.00*
<b><i>Acinetobacter</i></b>	6.99 ± 0.12	0.01 ± 0.01*	7.89 ± 0.63**	0.00 ± 0.00*
<i>Pseudomonas</i>	5.07 ± 0.49	0.52 ± 0.08*	6.20 ± 0.45**	0.52 ± 0.05*
<i>Unclassified_Firmicutes</i> <sup>†</sup>	1.61 ± 0.10	0.36 ± 0.45*	1.91 ± 0.09**	0.16 ± 0.01*
<i>Unclassified_Clostridiales</i> <sup>†</sup>	0.13 ± 0.01	0.06 ± 0.01*	0.17 ± 0.02**	0.06 ± 0.00*
<i>Unclassified_Clostridiaceae</i> <sup>†</sup>	0.05 ± 0.01	0.02 ± 0.00*	0.07 ± 0.01**	0.02 ± 0.00*
<i>Clostridium sensu stricto</i> <sup>†</sup>	0.06 ± 0.01	0.02 ± 0.00*	0.10 ± 0.03**	0.03 ± 0.00*
<b>60 kPa</b>				
<i>Micrococcus</i> <sup>†</sup>	0.04 ± 0.01	0.00 ± 0.00*	0.06 ± 0.00**	0.00 ± 0.00*
<i>Cloacibacterium</i>	0.10 ± 0.01	0.00 ± 0.00*	0.11 ± 0.01	0.01 ± 0.00*
<i>Paludibacter</i>	0.43 ± 0.04	0.13 ± 0.02*	0.50 ± 0.10	0.26 ± 0.28
<b><i>Acinetobacter</i></b>	7.13 ± 0.32	0.00 ± 0.00*	7.85 ± 0.18**	0.01 ± 0.02*
<i>Pseudomonas</i>	5.22 ± 0.18	0.51 ± 0.05*	5.93 ± 0.46**	0.52 ± 0.24*
<i>Unclassified_Firmicutes</i> <sup>†</sup>	1.79 ± 0.10	0.13 ± 0.03*	2.03 ± 0.18**	0.38 ± 0.44*
<i>Unclassified_Clostridiales</i> <sup>†</sup>	0.12 ± 0.00	0.07 ± 0.01*	0.15 ± 0.01**	0.07 ± 0.02*
<i>Unclassified_Clostridiaceae</i> <sup>†</sup>	0.04 ± 0.01	0.02 ± 0.00*	0.05 ± 0.01	0.02 ± 0.01*
<i>Clostridium sensu stricto</i> <sup>†</sup>	0.06 ± 0.00	0.02 ± 0.00*	0.06 ± 0.01	0.03 ± 0.01*

Only genera that changed in their relative abundance for all tested membranes were shown. \* and \*\* cells indicate statistically lower and higher relative abundance, respectively, compared to the control ( $P < 0.05$ ). Data are presented as average of biological replicates ( $n = 3$ ) ± SD. *Acinetobacter* in bold indicates the genus targeted by the bacteriophages used in this study.

<sup>†</sup>Genera that include gram-positive bacteria.

**Comparison with Chemical Treatment.** To compare the UV-C + bacteriophage treatment with the common chemical treatment used for membrane cleaning, we applied the two treatments against a membrane biofilm harvested at  $40 \pm 2$  kPa. The efficacy of both treatments was assessed based on the change in the cell number, ATP concentration, and protein and polysaccharide content. UV-C + bacteriophage treatment outcompeted the other tested treatments (i.e., bacteriophage and UV-C only) and was therefore further compared against the common chemical (i.e., sodium hypochlorite and citric acid) cleaning process. Both UV-C + bacteriophage and chemical treatment significantly reduced the values of all the biofilm parameters examined, namely, cell number, ATP concentration, alive and dead cells ratio, and protein and polysaccharides concentration, compared to the control ( $P < 0.0001$ ; Fig. 4 and S9). However, ATP concentration was not significantly different between UV-C + bacteriophage and chemical treatment ( $P = 0.35$ ). Log cells reduction compared with the control was slightly different between chemical treatment and UV-C + bacteriophage treatment ( $1.7 \pm 0.2$  and  $1.4 \pm 0.3$ , respectively,  $P = 0.04$ ) (Fig. 4A). Moreover, the value of the ratio of alive and dead cells upon chemical treatment was 0.2, while the one after UV-C + bacteriophage treatment was 0.4 (SI Appendix, Fig. S9;  $P = 0.02$ ). In addition, the chemical treatment method was 4 to 6× more effective in reducing proteins and polysaccharides concentration in biofilm matrix compared to UV-C + bacteriophage treatment (Fig. 4B;  $P < 0.0001$ ).

## Discussion

In our study, we used *Acinetobacter* genus, specifically *A. modestus*, *A. junii*, and *A. seohaensis* as model microorganisms to be targeted by bacteriophages as a way to alleviate membrane fouling in an AnMBR. Genus *Acinetobacter* is facultative anaerobe and is able to reach 3 to 4% of the total microbial community present on the membrane (31). Using these three *Acinetobacter* species, we isolated three bacteriophages from the *Podoviridae* family. We observed that bacteriophage infection alone can impact the biofilm community only with certain extent of membrane biofouling. For instance, when membrane was harvested at TMP of ca. 40 and 60 kPa, bacteriophage mixture application resulted in <1-log reduction of bacterial cells, ATP concentration (Fig. 1), and alive and dead cell ratio (Table 1) from the biofilm. This observation is in agreement with the earlier studies that also reported the addition of bacteriophages to membrane-associated single-species biofilm led to a 40% reduction of attached cells (25) and 70% flux recovery (23).

However, when membranes harvested at  $20 \pm 2$  kPa (i.e., at early stages of fouling) were treated with bacteriophage mixture, the bacteriophages were not able to propagate to numbers that would significantly impact membrane biofouling (Fig. 1 and SI Appendix, Fig. S7). This poor effect may be due to a low number of *Acinetobacter* present within the membrane biofilm. It was previously observed that regardless of the number of bacteriophages present in the system, a density of  $10^6$  CFU/mL of the target bacterial cells or an optimal MOI is necessary to ensure an

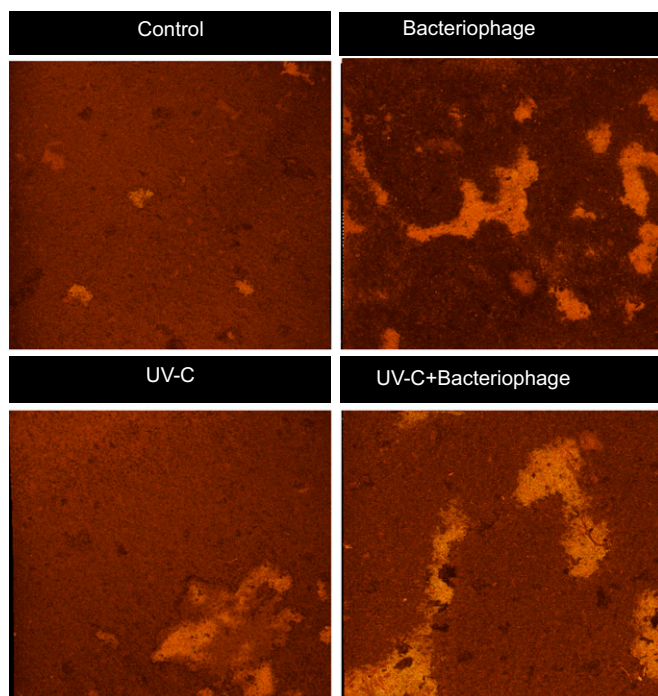


**Fig. 3.** Upper view of 3D OCT scans of the membrane biofilm for control and the three treatments. Darker color indicates thicker biofilm, while brighter color represents areas not covered by biofilm. The area visualized is  $8 \times 8$  mm.

efficient phage–bacteria interaction and to initiate phage infection (34). Although *Acinetobacter* spp. was considered a core component of biofilm structure in AnMBR (31), it is likely that the total number of *Acinetobacter* spp. within a young biofilm was not enough to initiate an effective infection. For the same reason, at

$20 \pm 2$  kPa, the removal of protein and polysaccharide was also minimal. The reduction of the EPS component of the biofilm may be due to the dislocation effect resulted from the bacteriophage action and to the possible release of enzymes that disrupt this fraction. Naturally, if an effective biofilm infection does not occur, the impact on the EPS would be minimal. On the contrary, the reduction in the number of cells and EPS in the biofilm was maximum at medium biofouling rate ( $40 \pm 2$  kPa). Membrane biofilm harvested at  $40 \pm 2$  kPa showed the highest cell activity compared with the other biofouling rates (Fig. 1B). High host activity is a crucial trait that favors phage infection since bacteriophages use host machinery to replicate and to propagate inside the cell (35). Instead, at  $60 \pm 2$  kPa, even if the *Acinetobacter* population was likely higher in abundance than that at  $40 \pm 2$  kPa, the thicker biofilm structure might have inhibited the bacteriophage penetration and therefore the phage–cell interaction.

It was observed that phage alone, regardless of whether it was used to target a single species biofilm or a complex biofilm like that in this study, did not result in a significant eradication of membrane foulants compared to the control. We therefore further proposed the combination of bacteriophages and UV-C irradiation as an enhanced membrane cleaning approach. We observed that both the bacteriophages and UV-C acted synergistically to disrupt the biofilm matrix and to enhance cell removal compared with either of the individual treatment. The mechanism behind this synergism is speculated to be achieved via two steps. First, UV-C may act on the whole bacterial community by killing the bacteria and loosening the biofilm matrix. Bacteria exposed to UV-C lose their ability to replicate which led to cell death (36). In earlier studies, UV-C irradiation was used as pretreatment to reduce biofouling in wastewater treatment both alone or in combination with chlorine (27, 37). Moreover, when it was applied as antibiofilm agent (38, 39), the cell log reduction was in agreement with that observed in our study. UV-C can therefore lead to these dead cells being dislodged from the membrane surface which was observed from the OCT analysis

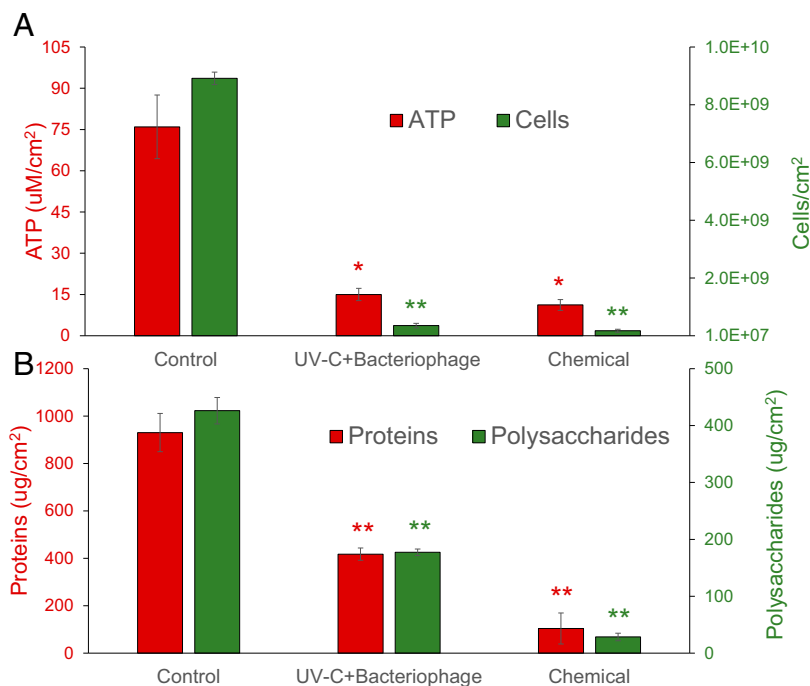


**Fig. 4.** (A) ATP concentration and cell number and (B) protein and polysaccharide concentration in membrane biofilm in control, UV-C + bacteriophages mixture treatment, and chemical addition. The biofilm was collected at a TMP of 40 kPa. Error bars indicate SD among the three replicates. For each condition, an asterisk indicates that the value is statistically different compared with the control, while two asterisks indicate that the value is statistically different compared with control and with the other condition.



(40, 41), in which cavities within the biofilm matrix were characterized by a lower biofilm coverage and a reduction of thickness and biovolume compared with the control (Fig. 3).

Second, by loosening the biofilm matrix, bacteriophages are now able to penetrate deeper into the biofilm to infect the intended hosts embedded nearer to the membrane surface. Interestingly, UV-C + bacteriophages not only affected relative abundance of *Acinetobacter* but also that from other non-*Acinetobacter* spp. (Table 2). The reduction of *Paludibacter*, *Pseudomonas*, *Cloacibacterium*, and gram-positive Firmicutes may not be due to a direct infection by the phages but rather due to a variety of phage proteins such as holins, endolysin, and spanins that can act on other microorganisms, particularly on the gram-positive bacteria outer membrane (42). In addition, some bacteriophages also encode for enzymes that damage the EPS, which would disrupt the biofilm matrix (21). Pairing UV-C with bacteriophages can also trigger the latter into lytic mode (35, 43), as is exemplified from the reduced membrane cleaning efficiency when bacteriophages were introduced independently from UV-C (SI Appendix, Fig. S8). Our results showed that this additive effect was particularly optimal when membranes were subcritically fouled at  $40 \pm 2$  kPa (Fig. 1), with a higher number of evaluated genus showing a reduction in the relative abundance compared to that observed at other TMPs (Table 2).

Despite this positive result of the UV-C + bacteriophages treatment, the approach has to be optimized in terms of UV irradiation intensity. From our results, only *A. modestus* bacteriophage was able to effectively propagate when it was coupled with UV-C irradiation. On the contrary, the other two bacteriophages reduced in terms of PFU compared with the initial number and hence may have hindered the overall infection efficacy. Varying susceptibilities toward UV-C among the three bacteriophages could be due to differences in GC content of phage genome since UV-C induces formation of covalent linkages among pyrimidine bases (e.g., uracil or cytosine) that leads to cell death (44). Alternatively, it could also be due to differences in the abundance of the host bacterial species within the biofilm matrix that led to different infectivity and propagation rates among the three phages. Optimization of the irradiation intensity to maximize the antifouling effect and minimize detrimental impact on the bacteriophages and the associated energy demands of UV-C lamps would represent a crucial step to allow the applicability of this approach at a larger scale.

Furthermore, when translating this approach to full-scale applications, it is important to note that the combined UV-C + bacteriophage approach was less effective in reducing protein and polysaccharides concentration in biofilm matrix when compared with the sodium hypochlorite and citric acid cleaning (Fig. 4B). Sodium hypochlorite and citric acid are commonly used to clean fouled membranes. Sodium hypochlorite is a strong oxidant that modifies the cell membrane permeability by reacting with phospholipids (45). Citric acid chelates inorganic minerals and disrupts the stability of the biofilm matrix (46, 47). Therefore, while chemical cleaning is directed to the removal of biofilm EPS and irreversible foulant layer, UV-C and bacteriophages may be more useful against reversible foulants formed during the medium stages of fouling (e.g., at TMP of  $40 \pm 2$  kPa). The proposed UV-C + bacteriophage approach is also only applicable for use in external configured membrane units or in second-stage membrane holding tanks that do not have high mixed liquor suspended solids (MLSS) concentration since turbidity will result in poor UV-C efficacy. Bacteriophages will also need to be maintained as a side culture to meet the operational demands. Although this study demonstrated the use of MOI 1 to achieve an efficient removal of membrane biofoulants, it is likely that lower MOI of 0.01 or 0.1 would also achieve a similar efficacy since there was no difference in the specific growth rates of *Acinetobacter* hosts at these MOIs (SI

Appendix, Fig. S6). The use of a lower MOI in actual applications would bring down the associated costs needed to maintain the bacteriophages as side cultures.

Recognizing the strengths and limitations of our proposed approach, we envision that the UV-C + bacteriophage cleaning approach can possibly be carried out in a semicontinuous mode with minimal downtime to the operation since bacteriophages are already capable of reducing biofilm thickness and biovolume after 1 h of application (SI Appendix, Table S3). In this mode, filtration to an externally configured or second-stage membrane tank (in which MLSS is controlled to a level that does not compromise UV-C penetration and efficacy) can be momentarily paused to allow membrane exposure to UV-C and bacteriophages. At the end of the treatment, the membrane could be backwashed to remove the phages from the surface before resuming the normal filtration process. This strategy could potentially delay the occurrence of membrane fouling by removing the reversible fouling layers developed on membranes, in turn reducing the frequencies and amount of chemicals needed throughout the course of operation. However, a techno-economic assessment would need to be done to determine the overall energy costs associated with our proposed cleaning strategy and how it would compare against the conventional cleaning approaches. Finally, although this proof of concept is only demonstrated on AnMBR in this study, the same approach can also be applied to other membrane-based technologies (e.g., desalination and aerobic membrane bioreactors) as long as the core keystone bacterial groups are already identified and the associated phages targeting these bacterial groups are isolated and propagated for subsequent use. Further studies to optimize the paired use of UV-C and bacteriophage to clean membranes in full-scale systems would also be needed.

## Materials and Methods

**Bacteriophages Isolation and Characterization.** *A. junii*, *A. modestus*, and *A. seohaensis* were isolated from wastewater during our routine wastewater monitoring surveillance. Considering the presence of these three species representing *Acinetobacter* genus in wastewater, bacteriophages targeting them were subsequently isolated from the influent of the KAUST wastewater treatment plant as described before (22) and propagated by the double-layer method (48). A detailed description of bacteriophages isolation can be found in SI Appendix, Bacteriophages Isolation.

Phage morphology was characterized by transmission electron microscopy (TEM) (Tecnai Spirit TWIN, FEI) operated at 120 kV and equipped with an ORIUS SC1000 camera (Gaitan). To obtain TEM photos, the three bacteriophages in suspension were first fixed with 2.5% vol/vol glutaraldehyde and then placed on carbon-coated copper grids before being negatively stained with 1% wt/vol uranyl acetate.

**Reactor Setup and Operations.** AnMBR configuration (SI Appendix, Fig. S5A) used was similar to the one in earlier study (49). A 2-L reactor, operated without air sparging, was filled with ceramic rings to support biofilm establishment, and it was inoculated with the same seed sludge described elsewhere (8). Synthetic wastewater with a COD of 750 mg/L was fed into the reactor with a hydraulic retention time of 18.5 h. The reactor was operated at pH 7 and at 35 °C, and no sludge was wasted during the entire study. The reactor was connected externally to three PVDF microfiltration membrane (0.3 μm nominal pore size, GE Osmonics) modules in parallel. The three external membranes were operated in cross-flow mode with stable flux that ranged from 6 to 7 L/m<sup>2</sup>/h. Biogas was used to scour the membrane surface. The three membranes served as biological replicates for the experiments. TMP was recorded every day by a pressure gauge connected to each membrane module. Following the indication of a previous study (49), membranes were harvested, treated *ex situ*, and analyzed at three different TMP values, i.e.,  $20 \pm 2$ ,  $40 \pm 2$ , and  $60 \pm 2$  kPa, which represent increasing biofouling extent (SI Appendix, Fig. S5B). Three biological replicates of fouled membranes were harvested at each TMP value.

**Membrane Harvesting and Treatment Application.** Harvested membranes were processed for analysis. The first 3 cm at each end of the membranes were discarded because biofilm formation was not homogenous at those locations.

More information on how the homogeneity of the membrane biofilm was assessed is present in *SI Appendix, Membrane Biofilm Homogeneity*. The rest of the membrane, with homogenous biofilm, was cut into four pieces with dimensions 2 × 2 cm. These pieces were individually placed in small sterile Petri dish that contained 1× phosphate buffer solution (PBS) and subsequently incubated at room temperature for 6 h. Before the incubation, three types of treatments were applied, namely, 1) bacteriophage mixture treatment, named “bacteriophage,” with a total MOI of 1; 2) UV-C treatment, by exposing the biofilm to 100 mJ/cm<sup>2</sup> twice, at 3 and 6 h from the start of the incubation; and 3) a combination of the three *Acinetobacter* bacteriophages at an MOI of 1 and UV-C irradiation exposing the biofilm to 100 mJ/cm<sup>2</sup> twice, at 3 and 6 h from the start of the incubation (this treatment was named “UV-C + bacteriophage”). A last treatment involves UV-C being applied before bacteriophages addition in an independent manner (this treatment was named “independent UV-C + bacteriophage,” and more details are provided in *SI Appendix, Effect of UV-C and Bacteriophages Application Order*). Last, one piece of membrane was soaked in 1× PBS for 6 h to represent control. The bacteriophage MOI was set based on the relative abundances of *Acinetobacter* spp. observed in a previous study (31). More information on how the MOI value was selected can be found in *SI Appendix, MOI Value Setting*.

At the end of the 6 h, 1 mL of the solution in which the membrane was soaked was aliquot for PFU counting as described in the next section. Afterward, the membrane piece was removed from the solution, washed, and placed in fresh 1× PBS. Biomass attached on membrane was dislodged into the solution by sonication for 5 min using a Q500 sonicator (Qsonica) at 25% amplitude with 5-s pulsating step. The rest of the biofilm that remained tightly adhered on the membrane was scraped using a sterile inoculation loop. Both dislodged and scraped biomass in solution are combined to constitute the suspended biofilm biomass solution. The suspended solution was then used to enumerate the total cells, the ratio between alive and dead cells, and the proteins and polysaccharides concentration. Biological triplicates were performed for each treatment.

**Bacteriophages Plaque Counts after the Treatments.** The 1-mL aliquot was filtered through 0.22- $\mu$ m syringe filter to remove remaining biomass. Several dilutions, ranging from 10<sup>-1</sup> to 10<sup>-4</sup>-fold were performed in sodium magnesium buffer (5.8 g/L NaCl, 0.975 g/L MgSO<sub>4</sub>, 50 mL/L 50 mM Tris-Cl at pH 7.5), and 10  $\mu$ L of the diluted suspension was mixed individually with 100  $\mu$ L of *A. junii*, *A. modestus*, and *A. seohaensis* cultures. The presence of plaques was identified with the double-layer method (48), and it was compared with the initial amount of PFU/mL of each bacteriophage spiked for the treatments (5.4 × 10<sup>7</sup> PFU/mL of *A. junii* bacteriophage, 6.9 × 10<sup>7</sup> PFU/mL of *A. modestus* bacteriophage, and 2.1 × 10<sup>6</sup> PFU/mL of *A. seohaensis* bacteriophage). Plaque count for each treatment was performed in biological triplicates.

**Biofilm Characterization.** Biofilm structure was characterized by enumerating the total cells, the proportion of cells with intact cell wall membranes, adenosine triphosphate (ATP) concentration, and EPS concentration. Biological triplicates were performed for each treatment.

To enumerate cells, membrane biofilm suspension from the harvested membrane was diluted by 10<sup>4</sup>, stained with SYBR green (Thermo Fisher Scientific) for 15 min at 37 °C, and counted using a BD Accuri flow cytometer (BD Bioscience). The ratio between alive and dead cells was calculated by staining the same diluted biofilm suspension using the LIVE/DEAD BacLight Bacterial Viability and Counting kit (Thermo Fisher Scientific) for 15 min in the dark at room temperature. Alive and dead cells were enumerated using a BD Accuri flow cytometer (BD Bioscience). ATP concentration was measured using a Celsis ATP reagent kit and an Advance luminometer (Celsis).

For EPS analysis, both polysaccharide and protein concentrations were measured as described in a previous study (50). First, 2 mL of biofilm suspension was filtered through 0.22- $\mu$ m syringe filter to quantify only the filtrate (i.e., dissolved constituents). For each piece of cut membrane, total protein concentration was measured in triplicates by Total Protein kit (Sigma-Aldrich) using bovine serum albumin (BSA) as standard (Sigma-Aldrich). Finally, polysaccharides were quantified by the phenol-

sulfuric method (51), using glucose as standard (Sigma-Aldrich). Briefly, 1 mL of each sample (including different concentrations of glucose standard) was mixed with 1 mL of 5% vol/vol phenol solution and with 5 mL 98% sulfuric acid (Sigma-Aldrich). The mixture was incubated at room temperature for 20 min before measuring optical density at 490 nm.

**RNA Extraction and Biofilm Microbial Community Analysis.** To analyze the composition of the active biofilm bacterial community, an aliquot of 3 mL of suspended biofilm biomass was used to extract the RNA that was then reverse transcribed into first-strand complementary DNA. The 16S rRNA gene amplicon sequencing was performed to assess the influence of the different treatment on the membrane biofilm community as described before (52–54). More details can be found in *SI Appendix, RNA Extraction and Amplicon Sequencing Analysis*. All high-throughput sequencing files were deposited in the archive of the European Nucleotide Archive under study accession no. PRJEB38595.

**OCT Analysis.** A spectral domain OCT SD-OCT system device (Ganymede I, Thorlabs GmbH) provided with LSM03 scan lens was employed to non-invasively evaluate the effect of the treatments on the biomass developed on the membrane surface. The OCT employs backscattered light to acquire cross-sectional scans of membrane. A membrane module connected to the same AnMBR used in the earlier experiments was operated to reach a TMP of 40 ± 2 kPa. This TMP value was chosen because it resulted in the best biofilm removal for the three treatments compared with the control. The membrane was therefore harvested at TMP of 40 ± 2 kPa and cut to four pieces for individual application of the three treatments (i.e., bacteriophage, UV-C, and UV-C + bacteriophage), with the remaining portion used as nontreated control. At the end of the 6-h treatment, the membrane pieces in the Petri dish were positioned under the OCT probe to assess the efficiency of each treatment in removing the biomass from the membrane surface. Three-dimensional images for each analysis were obtained to show and visualize the biofouling reduction. In addition, a time series analysis was performed to monitor the effect of the bacteriophage treatment alone by fixing the membrane coupons under the OCT probe.

The biomass morphology descriptors, namely, biovolume, biofilm coverage, average thickness, and the relative roughness, were calculated using the equation reported in literature (40, 41), by analyzing 500 scan images for the 3D scan. More details can be found in *SI Appendix, OCT Images Analysis*.

**Comparison with Chemical Membrane Cleaning.** We further compared the UV-C + bacteriophage treatment to the conventional cleaning process. Briefly, a membrane module connected to the same AnMBR used for the previous experiments was harvested at TMP of 40 ± 2 kPa and cut into three pieces of dimension 2 × 2 cm. The pieces were individually placed in a small Petri dish filled with 1× PBS. One of these pieces was exposed to the same mixed treatment described above (UV-C + bacteriophages), the second piece was soaked in a mixture of 0.1 M citric acid and 6% sodium hypochlorite solution, and the last piece of membrane was used as control submerged in 1× PBS.

After 6 h, the membrane was removed from the solution, and the biofilm was resuspended in fresh 1× PBS as described before. The experiment was performed in triplicates. The effect of the two different treatments compared to the control was examined with the same analysis described in *Biofilm Characterization*.

**Statistical Analysis.** Statistical differences for the parameters at different conditions were evaluated through one-way ANOVA with significance level set at 95% confidence level ( $P < 0.05$ ).

**Data Availability.** All study data are included in the article and *SI Appendix*.

All high-throughput sequencing files were deposited in the archive of the European Nucleotide Archive under study accession no. PRJEB38595.

**ACKNOWLEDGMENTS.** This study was supported by KAUST Center Applied Research Funding FCC/1/1971-32-01 and Center of Excellence for NEOM Research Flagship Projects REI/1/4178-03-01 awarded to P.-Y.H.

1. A. L. Smith, L. B. Stadler, N. G. Love, S. J. Skerlos, L. Raskin, Perspectives on anaerobic membrane bioreactor treatment of domestic wastewater: A critical review. *Bioresour. Technol.* **122**, 149–159 (2012).
2. C.-H. Wei, M. Harb, G. Amy, P.-Y. Hong, T. Leiknes, Sustainable organic loading rate and energy recovery potential of mesophilic anaerobic membrane bioreactor for municipal wastewater treatment. *Bioresour. Technol.* **166**, 326–334 (2014).
3. D. Rosso, M. K. Stenstrom, L. E. Larson, Aeration of large-scale municipal wastewater treatment plants: State of the art. *Water Sci. Technol.* **57**, 973–978 (2008).
4. A. L. Prieto, H. Futselaar, P. N. Lens, R. Bair, D. H. Yeh, Development and start up of a gas-lift anaerobic membrane bioreactor (GI-AnMBR) for conversion of sewage to energy, water and nutrients. *J. Membr. Sci.* **441**, 158–167 (2013).
5. B.-Q. Liao, J. T. Kraemer, D. M. Bagley, Anaerobic membrane bioreactors: Applications and research directions. *Crit. Rev. Environ. Sci. Technol.* **36**, 489–530 (2006).



6. M. Maaz *et al.*, Anaerobic membrane bioreactors for wastewater treatment: Novel configurations, fouling control and energy considerations. *Bioresour. Technol.* **283**, 358–372 (2019).
7. M. Harb, P.-Y. Hong, Anaerobic membrane bioreactor effluent reuse: A review of microbial safety concerns. *Fermentation (Basel)* **3**, 39 (2017).
8. Y. Xiong, M. Harb, P.-Y. Hong, Characterization of biofouling illustrates different membrane fouling mechanisms for aerobic and anaerobic membrane bioreactors. *Separ. Purif. Tech.* **157**, 192–202 (2016).
9. P. Xu, J. E. Drewes, T.-U. Kim, C. Bellona, G. Amy, Effect of membrane fouling on transport of organic contaminants in NF/RO membrane applications. *J. Membr. Sci.* **279**, 165–175 (2006).
10. A. McWilliams, *Membrane Bioreactors: Global Markets* (BCC Research, 2019), pp. 168.
11. D. P. Thanu, M. Zhao, Z. Han, M. Keswani, "Fundamentals and applications of sonic technology" in *Developments in Surface Contamination and Cleaning: Applications of Cleaning Techniques*, R. Kohli, K. L. Mittal, Eds. (Elsevier, 2019), pp. 1–48.
12. M. Ayub, N. Saeed, S. Chung, M. S. Nawaz, N. Ghaffour, Physical and economical evaluation of laboratory-scale membrane bioreactor by long-term relative cost-benefit analysis. *J. Water Reuse Desalin.* **10**, 239–250 (2020).
13. X. Shi, G. Tal, N. P. Hankins, V. Gitis, Fouling and cleaning of ultrafiltration membranes: A review. *J. Water Process Eng.* **1**, 121–138 (2014).
14. K. Kimura, Y. Hane, Y. Watanabe, G. Amy, N. Ohkuma, Irreversible membrane fouling during ultrafiltration of surface water. *Water Res.* **38**, 3431–3441 (2004).
15. M. R. Jumat, M. F. Haroon, N. Al-Jassim, H. Cheng, P.-Y. Hong, An increase of abundance and transcriptional activity for *Acinetobacter junii* post wastewater treatment. *Water* **10**, 436 (2018).
16. Y. Xiong, Y. Liu, Biological control of microbial attachment: A promising alternative for mitigating membrane biofouling. *Appl. Microbiol. Biotechnol.* **86**, 825–837 (2010).
17. L. Malaeb, P. Le-Clech, J. S. Vrouwenvelder, G. M. Ayoub, P. E. Saikaly, Do biological-based strategies hold promise to biofouling control in MBRs? *Water Res.* **47**, 5447–5463 (2013).
18. K. S. Liao, S. M. Lehman, D. J. Twardy, R. M. Donlan, B. W. Trautner, Bacteriophages are synergistic with bacterial interference for the prevention of *Pseudomonas aeruginosa* biofilm formation on urinary catheters. *J. Appl. Microbiol.* **113**, 1530–1539 (2012).
19. D. Alemayehu *et al.*, Bacteriophages  $\phi$ MR299-2 and  $\phi$ NH-4 can eliminate *Pseudomonas aeruginosa* in the murine lung and on cystic fibrosis lung airway cells. *MBio* **3**, e00029–e12 (2012).
20. D. P. Pires, D. Vilas Boas, S. Sillankorva, J. Azeredo, Phage therapy: A step forward in the treatment of *Pseudomonas aeruginosa* infections. *J. Virol.* **89**, 7449–7456 (2015).
21. D. R. Harper *et al.*, Bacteriophages and biofilms. *Antibiotics (Basel)* **3**, 270–284 (2014).
22. G. Scarascia, S. A. Yap, A. H. Kaksonen, P.-Y. Hong, Bacteriophage infectivity against *Pseudomonas aeruginosa* in saline conditions. *Front. Microbiol.* **9**, 875 (2018).
23. A. S. Bhattacharjee, J. Choi, A. M. Motlagh, S. T. Mukherji, R. Goel, Bacteriophage therapy for membrane biofouling in membrane bioreactors and antibiotic-resistant bacterial biofilms. *Biotechnol. Bioeng.* **112**, 1644–1654 (2015).
24. W. Ma, M. Panecka, N. Tufenkji, M. S. Rahaman, Bacteriophage-based strategies for biofouling control in ultrafiltration: In situ biofouling mitigation, biocidal additives and biofilm cleanser. *J. Colloid Interface Sci.* **523**, 254–265 (2018).
25. G. Goldman, J. Starosvetsky, R. Armon, Inhibition of biofilm formation on UF membrane by use of specific bacteriophages. *J. Membr. Sci.* **342**, 145–152 (2009).
26. R. Gehr, M. Wagner, P. Veerasubramanian, P. Payment, Disinfection efficiency of peracetic acid, UV and ozone after enhanced primary treatment of municipal wastewater. *Water Res.* **37**, 4573–4586 (2003).
27. A. Benito, G. Garcia, R. Gonzalez-Olmos, Fouling reduction by UV-based pretreatment in hollow fiber ultrafiltration membranes for urban wastewater reuse. *J. Membr. Sci.* **536**, 141–147 (2017).
28. N. Pozos, K. Scow, S. Wuertz, J. Darby, UV disinfection in a model distribution system: Biofilm growth and microbial community. *Water Res.* **38**, 3083–3091 (2004).
29. Y. Zhu *et al.*, Characterization of biofilm and corrosion of cast iron pipes in drinking water distribution system with UV/Cl<sub>2</sub> disinfection. *Water Res.* **60**, 174–181 (2014).
30. N. Trun, J. Trempy, *Fundamental Bacterial Genetics* (John Wiley & Sons, 2009).
31. H. Cheng, D. Cheng, J. Mao, T. Lu, P.-Y. Hong, Identification and characterization of core sludge and biofilm microbiota in anaerobic membrane bioreactors. *Environ. Int.* **133**, 105165 (2019).
32. H.-W. Ackermann, Classification of bacteriophages. *The bacteriophages* **635**, 8–16 (2006).
33. L. Fortunato, A. F. Lamprea, T. Leiknes, Evaluation of membrane fouling mitigation strategies in an algal membrane photobioreactor (AMPBR) treating secondary wastewater effluent. *Sci. Total Environ.* **708**, 134548 (2020).
34. S. Chibani-Chennoufi, A. Bruttin, M.-L. Dillmann, H. Brüssow, Phage-host interaction: An ecological perspective. *J. Bacteriol.* **186**, 3677–3686 (2004).
35. A. Campbell, The future of bacteriophage biology. *Nat. Rev. Genet.* **4**, 471–477 (2003).
36. N. Goosen, G. F. Moolenaar, Repair of UV damage in bacteria. *DNA Repair (Amst.)* **7**, 353–379 (2008).
37. J. Xing *et al.*, Application of low-dosage UV/chlorine pre-oxidation for mitigating ultrafiltration (UF) membrane fouling in natural surface water treatment. *Chem. Eng. J.* **344**, 62–70 (2018).
38. Y. M. Bae, S. Y. Lee, Inhibitory effects of UV treatment and a combination of UV and dry heat against pathogens on stainless steel and polypropylene surfaces. *J. Food Sci.* **77**, M61–M64 (2012).
39. C. Hadjok, G. S. Mittal, K. Warriner, Inactivation of human pathogens and spoilage bacteria on the surface and internalized within fresh produce by using a combination of ultraviolet light and hydrogen peroxide. *J. Appl. Microbiol.* **104**, 1014–1024 (2008).
40. L. Fortunato *et al.*, Cake layer characterization in activated sludge membrane bioreactors: Real-time analysis. *J. Membr. Sci.* **578**, 163–171 (2019).
41. L. Fortunato, N. Pathak, Z. U. Rehman, H. Shon, T. Leiknes, Real-time monitoring of membrane fouling development during early stages of activated sludge membrane bioreactor operation. *Process Saf. Environ. Prot.* **120**, 313–320 (2018).
42. R. Young, Phage lysis: Do we have the hole story yet? *Curr. Opin. Microbiol.* **16**, 790–797 (2013).
43. N. Al-Jassim, D. Mantilla-Calderon, G. Scarascia, P.-Y. Hong, Bacteriophages to sensitize a pathogenic New Delhi metallo- $\beta$ -lactamase-positive *Escherichia coli* to solar disinfection. *Environ. Sci. Technol.* **52**, 14331–14341 (2018).
44. W. A. Kowalski, P. B. William, M. T. Hernandez, A genomic model for the prediction of ultraviolet inactivation rate constants for RNA and DNA viruses. *IJVA News* **11**, 15–28 (2009).
45. G. Zhen *et al.*, Anaerobic membrane bioreactor towards biowaste biorefinery and chemical energy harvest: Recent progress, membrane fouling and future perspectives. *Renew. Sustain. Energy Rev.* **115**, 109392 (2019).
46. H. Lee *et al.*, Cleaning strategies for flux recovery of an ultrafiltration membrane fouled by natural organic matter. *Water Res.* **35**, 3301–3308 (2001).
47. N. Porcelli, S. Judd, Chemical cleaning of potable water membranes: A review. *Separ. Purif. Tech.* **71**, 137–143 (2010).
48. M. H. Adams, *Bacteriophages* (Interscience Publishers, Inc., 1959).
49. H. Cheng, P.-Y. Hong, Removal of antibiotic-resistant bacteria and antibiotic resistance genes affected by varying degrees of fouling on anaerobic microfiltration membranes. *Environ. Sci. Technol.* **51**, 12200–12209 (2017).
50. H. Cheng *et al.*, Antibiofilm effect enhanced by modification of 1,2,3-triazole and palladium nanoparticles on polysulfone membranes. *Sci. Rep.* **6**, 24289 (2016).
51. M. Dubois, K. A. Gilles, J. K. Hamilton, P. t. Rebers, F. Smith, Colorimetric method for determination of sugars and related substances. *Anal. Chem.* **28**, 350–356 (1956).
52. G. Scarascia, H. Cheng, M. Harb, P.-Y. Hong, Application of hierarchical oligonucleotide primer extension (HOPE) to assess relative abundances of ammonia- and nitrite-oxidizing bacteria. *BMC Microbiol.* **17**, 85 (2017).
53. R. C. Edgar, B. J. Haas, J. C. Clemente, C. Quince, R. Knight, UCHIME improves sensitivity and speed of chimera detection. *Bioinformatics* **27**, 2194–2200 (2011).
54. J. R. Cole *et al.*, The Ribosomal Database Project: Improved alignments and new tools for rRNA analysis. *Nucleic Acids Res.* **37**, D141–D145 (2009).